Probabilistic Approach to Assessing Capture System Performance Margin in Mars Sample Return's Capture, Containment, and Return System

Calinda M. Yew[1], Giuseppe Cataldo[2], Brendan Feehan[3], Eugenia De Marco[4]
NASA Goddard Space Flight Center, Greenbelt, MD, 20771, USA

George Antoun[5]
ATA Engineering, Inc., Lakewood, CO 80401

Elfego Pinon III[6]
Emergent Space Technologies, LLC; Laurel, MD 20707

In the aerospace industry, there are standard design principles and/or rule-of-thumb targets that define healthy levels of margins required at each developmental milestone for traditional metrics, such as mass, thermal, and power margins. When the technical resource is "non-traditional," in the sense that guiding margin principles are non-existent, systems engineering processes are required to internally generate performance targets and methodologies to assess the system against the derived targets. This paper presents a probabilistic approach for assessing complex time-critical operations which applies global sensitivity analyses to identify input parameters that should drive the design. This approach is used to design a critical payload required for the Mars Sample Return campaign aiming at bringing back rock and atmospheric samples from Mars.

I. Introduction

The Mars Sample Return (MSR) campaign, being developed jointly by NASA and the European Space Agency (ESA), aims to search for signs of ancient life on Mars by bringing samples of Martian rock, regolith (broken rock and dust), and atmosphere back to Earth[1-5]. To accomplish this, the baseline plan for the MSR campaign consists of four missions with separate key functions, as shown in Figure 1: the Mars 2020 Perseverance rover collects Martian samples and deposits them on the surface of Mars; the Sample Retrieval Lander (SRL) mission fetches the deposited samples, stores them in a protective vessel called the Orbiting Sample (OS) and launches it from the surface into Mars orbit; the Earth Return Orbiter (ERO) rendezvous with the OS in order to catch it, contain it, and bring it safely back to Earth; and finally, upon landing in the Utah Test and Training Range (UTTR), the Sample Receiving Project (SRP) is responsible for receiving and curating the samples for all the highly anticipated scientific investigations.

As one of the MSR campaign elements, the NASA-provided Capture, Containment, and Return System (CCRS) payload[6,7] on the ESA-provided Earth Return Orbiter (ERO) spacecraft[8] is responsible for several key capabilities for the campaign. The specific capability of OS capture is addressed in this paper. In the concept of operations for the capture function of the campaign, there are four main entities involved (Figure 2): the Mars Ascent Vehicle (MAV), the OS, the CCRS, and the ERO. The MAV launches from the surface and releases the OS containing the regolith samples into Mars orbit. The success of the mission hinges on the ability of the ERO to detect and rendezvous with the OS over the course of weeks to days and then position the CCRS to capture the OS in a process expected to take a matter of seconds. The CCRS project has a functional requirement that it *shall prevent the OS from exiting the capture volume after contact.*

[1] CCRS Capture & Configuration Phase Lead, Instrument & Payloads Systems Engineering Branch 592.
[2] CCRS Planetary Protection Lead, Planetary Protection, Contamination and Coatings Engineering Branch 546, AIAA Associate Fellow.
[3] CCRS Missions System Engineer, Missions Systems Engineering Branch 599.
[4] CCRS Capture & Configuration Product Design Lead, Mechanical Engineering Branch 543.
[5] Senior Technical Advisor, Rocky Mountain Operations.
[6] Senior Principal GN&C Engineer, Mission Engineering Division, AIAA Senior Member.

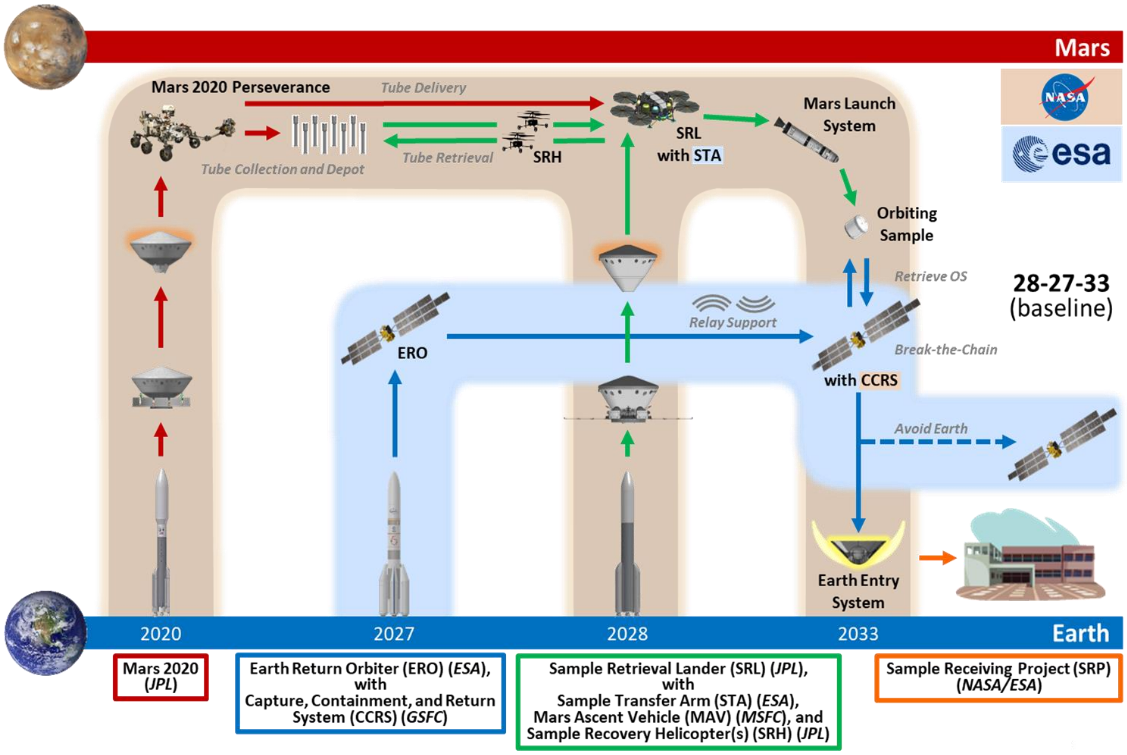

Figure 1. Mars Sample Return Campaign Planning Architecture

Although the requirement to capture the OS is not written in probabilistic terms, the verification thereof might require a probabilistic analysis approach. Not only is the CCRS assessment of its capture performance against this requirement dependent on several parameters outside its control, but the uncertainties in those parameters are broad and often ill-defined, especially in the preliminary design phases of the missions. Additionally, the problem becomes more complex to bound and assess when the four entities are out-of-phase in the project developmental life cycle. Figure 2 summarizes the external entities and the parameters within their control that directly impact the ability for CCRS to capture the OS. Each of the parameters has its own probability distribution and confidence level given where each project is in its developmental life cycle.

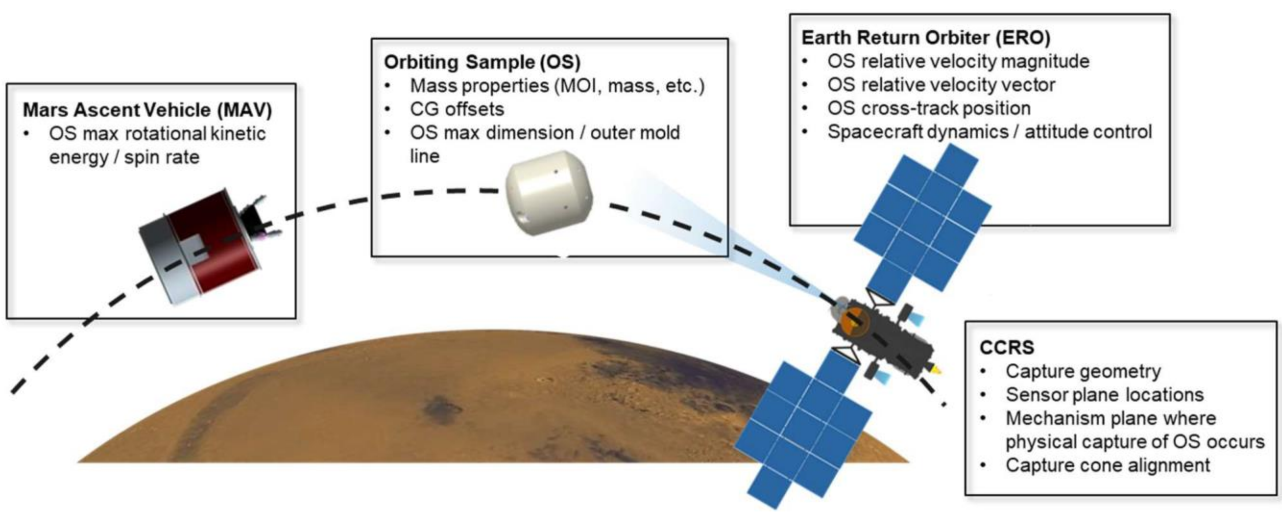

Figure 2. Input Parameters to CCRS Capture Performance

In the early phases of a project when simplified assessments dominate as the means to derive working numbers for detailed design (i.e., hardware sizing), the computations are often conservative by nature. As designs mature and uncertainties are refined, the hope is that the design still stands, and it usually does. Other times, unknown unknowns are uncovered, and the design changes required to accommodate the unknowns come at the expense of both technical resource constraints (i.e., mass, volume, etc.), and programmatic constraints (i.e., schedule, cost, etc.). When all the input parameters are stacked at their worst-case requirement bounds, which typically provides the first-order approximation that may be used in early design phases, it not only misrepresents the true distributions (and uncertainties) for each parameter, but it also produces an overly conservative result that may unnecessarily drive a mass-constrained system.

Adopting a stochastic (e.g., Monte Carlo) approach, therefore, to understand what input parameters ought to drive design changes in a highly constrained system becomes necessary in order to balance risk across all entities. This paper applies common probabilistic methods in order to define sufficient levels of margin, or system robustness, for time-based estimates of highly coupled relative dynamic problems. Margin for traditional technical resources, such as mass and power, are generally expressed in percent (e.g., 20% mass margin at preliminary design review). Rather than reporting metrics for CCRS' time-critical capture performance margins in terms of an absolute percentage of seconds, which provides very little indication of system robustness, this paper aims to: (1) report performance as the probability that the defined system capability limit will successfully execute and meet its capture requirement, and (2) apply a widely used global sensitivity analysis methodology and risk assessment to express capture margin as a sigma value to its most sensitive input parameter.

II. Overview of CCRS Capture Performance Definition

The CCRS has a dedicated capture volume to receive the OS at the conclusion of rendezvous, consisting of a cylindrical portion and a funnel portion. CCRS is blind to the exact time the OS enters the aperture of the capture volume and, thus, has implemented two light-emitting diode (LED) layers (called capture sensors) to detect the presence of the OS. The on-board CCRS avionics process the signals from the capture sensors to determine when the system should deploy a mechanism to capture the OS. The avionics implements the following high-level algorithm: obstruction of the upper LED layer or plane → obstruction of upper + lower LED layers → un-obstruction of upper LED layer + obstruction of lower LED layer. Once the OS has traversed below the upper capture sensor layer, it has cleared the plane of the mechanism used to physically trap the OS in the capture volume and, therefore, this is the start of the capture time budget, also designated as the "trigger time" for capture. Figure 3 shows key events for capture.

After the trigger time, the OS then continues into the capture volume, contacts a (random) point within the CCRS capture volume and bounces back towards the capture aperture to the plane of the mechanism used to capture the OS, called the Linear Transfer Mechanism (LTM). It is at the point when the OS bounces back to the plane of the LTM that the capture timing budget ends. The entire budget from trigger time until this ending point is termed the total capture-before-bounce-back budget, against which the CCRS system must perform to meet its functional requirement to prevent the OS from leaving the capture volume.

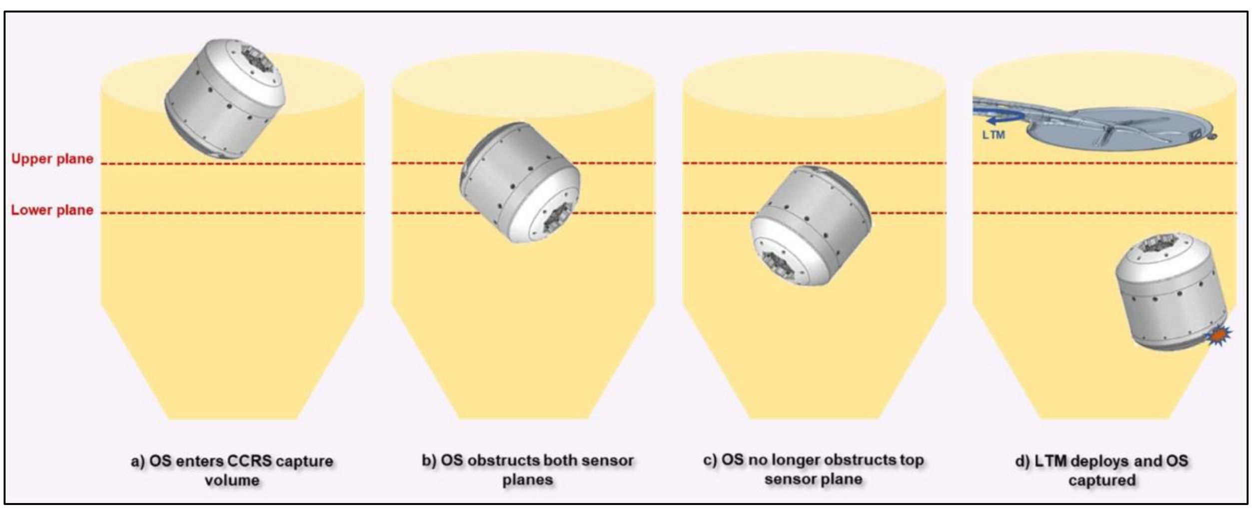

Figure 3. Capture Storyboard

Once capture is triggered (Figure 3c), the CCRS system has three hardware components that execute the closed-loop capture function within the capture-before-bounce-back budget. Table 1 provides the hardware component allocations, including a list of any uncertainties that are expected to be covered within the not-to-exceed (NTE) allocations for each subsystem.

Table 1. Capture-Before-Bounce-Back Timing Allocation

Item	Hardware Item	NTE Timing Allocation (s)	Description	Uncertainties
1	Capture sensor electronics (CSE)	0.10	• CSE processing for state determination	• Design changes (i.e., trade space for capture sensor locations, LTM pocket depth) thru Critical Design Review (CDR)
2	LTM swing arm	3.2	• Deploy LTM	• Performance as a function of temperature, workhorse actuator (WHA) input voltage, WHA torque/speed output, hinge resistive torques (i.e., lube viscosity), swung inertia maturity
3	Avionics	0.45	• Receive capture sensor statuses • Perform algorithm • Send command to deploy mechanism	• Algorithm uncertainties (i.e., persistence) • Data rate capabilities
CCRS System Total:		**3.75**	**System capability limit**	

Margins for the capture before-bounce-back timing are held at the subsystem, CCRS system, and ERO-CCRS/Sample Retrieval Lander (SRL)-CCRS missions-levels:

- Subsystem allocations are NTE values that are meant to absorb uncertainties in the design and subsystem performance. These NTEs are reflected in Table 1 and are used to set the system capability limit.
- CCRS system margin absorbs any internal design change that would impact the overall capture timing budget (i.e., capture volume changes, captures sensor plane locations, LTM plane, etc.); these design changes are outside the performance capability of each hardware component (which is covered in the previous bullet).
- Mission-level margins are codified through interface requirements between two or more projects. For instance, ERO controls the incoming OS rendezvous parameters (OS relative velocity magnitude, velocity vector, and lateral offset); there is margin held against these requirements, and since they are inputs to the capture margins, an understanding of the margins held across an interface becomes essential should CCRS system margins become insufficient, and negotiations between subsystems must ensue.

III. Applying the General Monte Carlo Process

A. Input Parameters and Distributions

In order to determine performance margins of the capture system, distributions for external parameters must be factored into the analysis and, thus, CCRS applies a Monte Carlo (MC) simulation[9] to identify probabilistic metrics for assessing end-to-end capture performance. The MC capture simulations are performed with commercial Multi-Body Dynamics analysis software, ADAMS, starting when the OS is at the entrance plane at the conclusion of rendezvous and ending after many impacts when the OS kinetic energy has dissipated. This model includes a component mode synthesis model of the CCRS capture volume geometry to accurately represent the local compliance and a rigid OS. Table 2 summarizes the randomized parameters and their respective distributions.

The first three input parameters shown in Table 2 are derived from MC runs performed by the ERO design team to characterize the expected conditions when the OS is at the CCRS entrance plane. At the end of the rendezvous segment, the ERO spacecraft approaches the OS from a position ahead of the orbital position of the OS, as shown in

Figure 4. The ERO guidance, navigation, and control (GNC) systems position the CCRS, located on top of the ERO spacecraft, so that the OS will cross the entrance plane as close to the central axis, labeled “Y_cap” in the figure, of the CCRS as possible. Due to the fact that the ERO thrusters are disabled for safety reasons at a point less than two meters from the OS and due to dispersions from GNC sensors and actuators, there could be some variability in the OS initial conditions, captured in the distributions for the first three inputs in Table 2.

Table 2. Monte Carlo Input Parameters and Distributions

#	Capture-before-bounce-back Input Parameter	Value [Requirement*]	Input Distribution for Monte Carlo Budget Derivation
System			
1	OS Velocity (cm/s)	4*	Fixed
2	OS Cross Track (cm)	≤10*	Gaussian distribution with 3 sigma at requirement values
3	OS Trajectory Angle (deg)	≤5*	Uniform distribution +/- 5 deg
4	OS Max Dimension (mm)	332	Assumes CG at centroid
5	OS CG Offset (mm)	±10 X_{OS}; ±5 radial*	Uniform CG, Uniform Offset
6	OS Max Rotational KE (J)	0.53*	Triangular distribution from 0-0.53J
7	OS MOI Ixx, Iyy/Izz (kg-m^2)	0.079, 0.091*	Fixed for 11.5kg OS
8	S/C dynamics (deg/sec)	±0.025*	Fixed rotation about S/C CG
9	OS Initial Orientation, 3 Euler angles (deg)	[0 360]	Uniform
	Time Before Bounce-back, from OS Cleared Upper Sensor Plane	6.09	Not a gaussian distribution, nonlinear model computed for each MC case based on first funnel/OMG impact location
10	Cone misalignment wrt capture axis (sec)	-0.1	Estimated
	Total Capture Budget:	**5.99**	

The primary outputs of interest from the MC simulation are: (a) the time of OS first impact; (b) the location of OS first contact; (c) the number of capture successes vs. failures. Failures from the MC are defined in two possible cases: (1) the OS does not make it into the capture volume, and (2) the OS bounces out before the system is able to deploy the LTM to physically cage it. To determine if the system capability limit for physically caging the OS falls within the allowable time before the OS bounces out, Eq. 1 can be used.

Total capture budget = time-until-contact from MC + bounce-back time computed as a fully elastic contact [Eq.1]

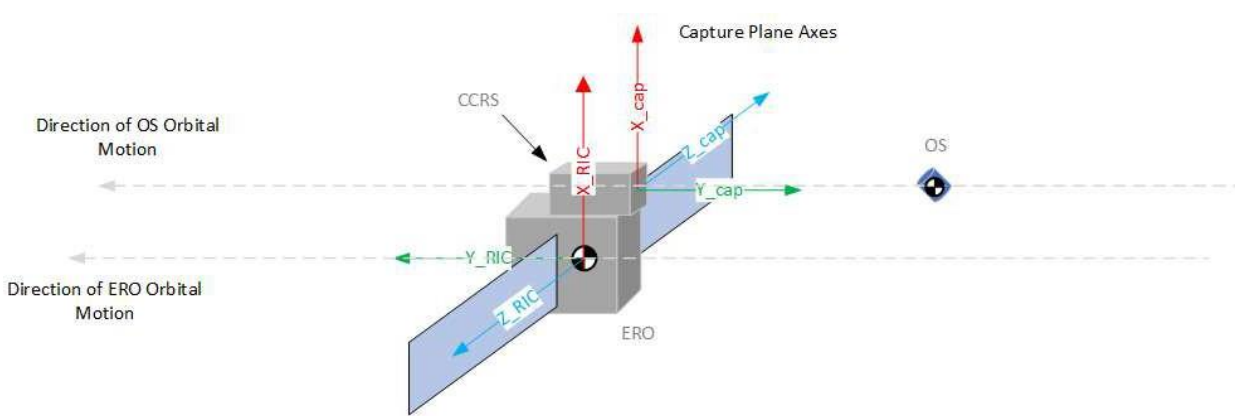

Figure 4. ERO Final Approach to Capture OS

B. Key and Driving Input Parameters

A global sensitivity analysis[10,11] using the primary outputs of the MC was used to identify the main drivers in the form of Sobol’ main indices. The Sobol’ main index measures the fraction of the total output variance that can be attributed to an input alone, whereas the total index measures the fraction of the total output variance that can be attributed to an input as well as its interactions with other inputs. Inputs with larger sensitivity indices contribute more to output uncertainty. Computing Sobol' indices for all inputs thus allows inputs to be ranked in terms of importance, enabling engineers to drop unimportant inputs for simplified analyses or to prioritize further characterization of important inputs to reduce the overall output uncertainty. Here, the Gamboa approach[12,13] was employed to compute the 17 Sobol' main indices and identify the OS cross-track error as the dominating parameter to which the capture timing is most sensitive with a Sobol' main index of 0.3. Sizing the opening diameter for the capture volume, therefore, uses the OS cross-track error as the design-to parameter; traditionally, a 3-sigma value is considered a sufficient design point, but the CCRS capture cone has been designed to the 3.8-sigma on the cross-track error. In terms of sizing of the capture volume length, the OS velocity and OS trajectory angle are the parameters to which that dimension is designed.

C. Derived Performance Targets

To set capture performance targets, engineering judgment must be used when there are no established guiding principles for the technical resource. The two driving factors that were considered in setting the performance metrics for CCRS capture and their associated targets are: (1) the uncertainties and threats to the performance, with extra emphasis on the parameters to which the system is most sensitive and (2) the level of acceptable risk with which the stakeholders are comfortable in a mission-critical, time-critical, operation. In consideration of these factors, the following capture performance metrics and targets were set for the system:

Table 3. Capture Performance Metrics and Targets

Metric	Metric Description	Target	Comments
1	**Percent System Margin for Capture Timing**	0.13% total capture-before-bounce-back has the following target margins: • 20% at Preliminary Design Review (PDR) • 15% at Critical Design Review (CDR) • 10% at Payload Delivery	Margin (in percent) = (Available Resource-Estimated Value of Resource)/Available Resource X 100 • Available resource = 0.13% first impact time • Estimated value of resource = system capability
2	**Probability of successful capture (P_s)**	≥99.7% success for 2,000 capture attempts (system capability $P_f \leq 0.3\%$)	Stakeholder / customer specification

The probability of successful capture metric requires a clear definition of what constitutes a successful capture. Capture success, therefore, has been defined with respect to two aspects of the CCRS design capabilities that, in conjunction, will meet the 99.7% target:

1. CCRS designs a capture volume that allows for successful OS entry, including:
    a. Sizing the capture volume to accommodate ERO rendezvous initial conditions of the OS at the entrance plane
    b. No inadvertent failure of the capture lid mechanism, which would block the OS entry into the cone
    c. No inadvertent failure of the LTM, which would also block the OS entry into the cone
2. CCRS designs the system to detect and cage the OS before it bounces out, such that each hardware item reliability complies to their allocations in Table 1: capture sensors detect the OS and transmit sensor state signals; the avionics performs the OS detection algorithm and sends the deployment command to the LTM mechanism; and the LTM deploys upon command.

The reliability of each component in Table 1 is used to compute the maximum probability of failure that the system capability limit would be allowed to lie on the MC output distribution. Independence between the component reliabilities can be assumed based on the fact that the failure of one component does not affect the failure of the others. Since the components function in series, meaning each must function for the system to work, the product rule for reliability applies:

$$P_{S(total)} = 99.7\% = P_{S(sensors)} * P_{S(avionics)} * P_{S(LTM)} * P_{S(MC)} \qquad \text{[Eq. 2]}$$

where,

$P_{S(total)}$ = total system probability of success
$P_{S(sensors)}$ = capture sensor component reliability / probability of success
$P_{S(avionics)}$ = avionics component reliability / probability of success
$P_{S(LTM)}$ = LTM deployment component reliability / probability of success
$P_{S(MC)}$ = minimum allowable probability of success for system capability (3.75 sec) on MC output distribution

$P_{S(MC)}$ can be derived from Eq. 2 and the associated $P_{f(MC)}$ is is allowable probability of failure for the MC output and is equivalent to $1 - P_{S(MC)}$. $P_{f(MC)}$ used to determine where the system capability of 3.75 sec can lie on the MC output distribution where the target $P_{f(max)}$ of 0.3% should be $\geq P_{f(MC)}$.

IV. Results

The MC results used for CCRS Preliminary Design Review (PDR) and shown in Figure 5 are based on the randomized parameters in accordance with the distributions indicated in Table 2. The results indicate that there are sufficient capture performance margins with respect to the timing target specified in Table 3. Additionally, results imply that the probability of success is sufficient to meet the target probability of at least 99.7%. Figure 5 provides the 2,000-case MC histograms representing: (a) the time of first impact with respect to the trigger time; (b) the location of first impact; (c) the associated impact distance along the length of the cone; (d) the bounce-back time; and finally (e) total capture-before-bounce-back time. The bounce-back time represented in Figure 5d was computed for each MC-case:

- Compute clearance between trailing edge of OS at instant of first impact (Figure 5c) and the LTM plane, D_ltm
- Compute max translational velocity, Vt_max, assuming no energy loss and initial kinetic energy, KE: Vt_max = sqrt(KE*2/mass)
- Bounce-back time = D_ltm/Vt_max, assumes all incoming kinetic energy converted to translation and rebounds directly along capture cone longitudinal axis

The total capture time (Figure 5e) is the addition of the time of first impact with respect to trigger (Figure 5a) and bounce-back time (Figure 5d).

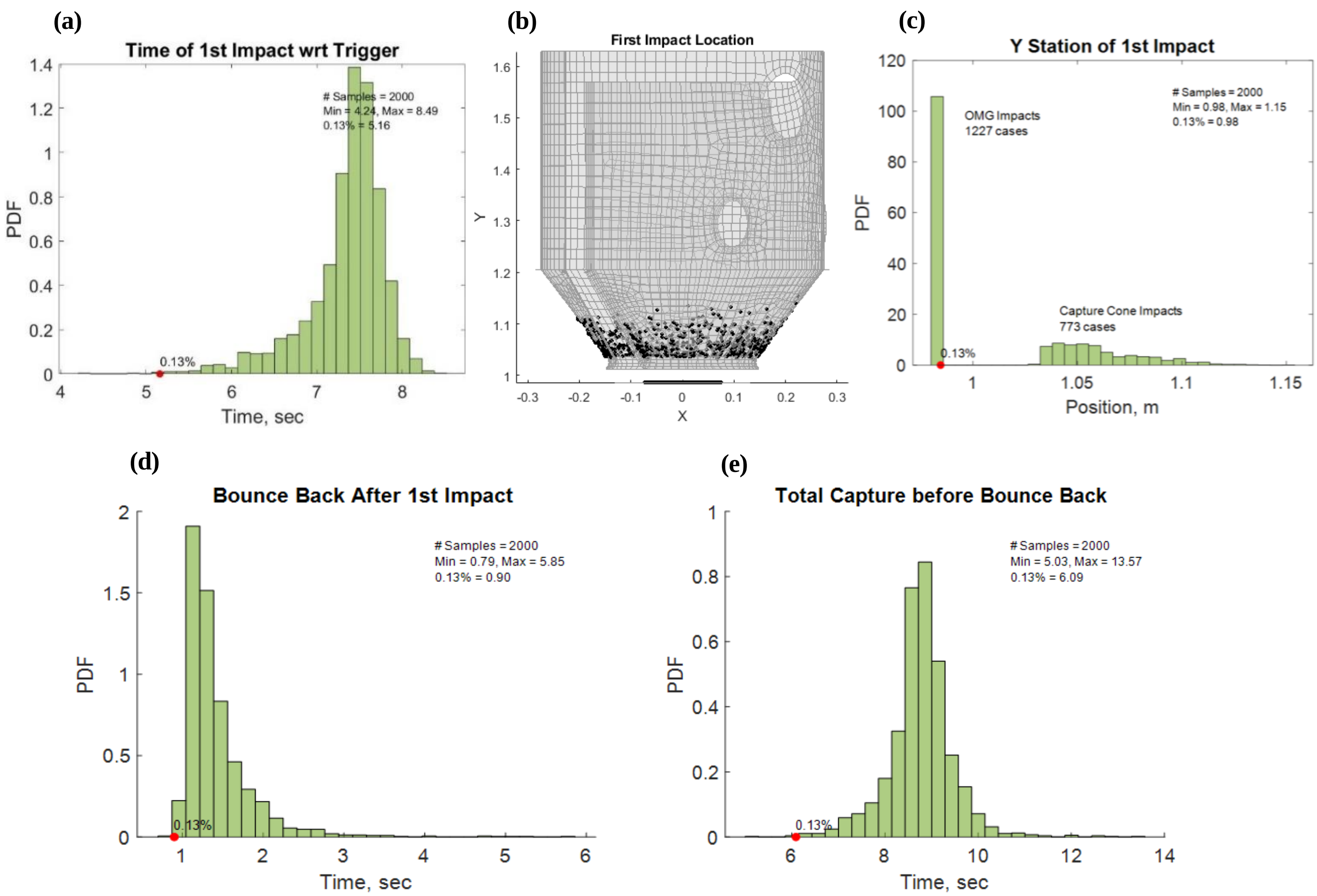

Figure 5. MC Histograms

A summary of the CCRS PDR capture performance results with respect to the project-derived target metrics is provided in Table 7. For metric 1, the current best estimate (CBE) timing performance for each hardware component is compared against their respective allocations in Table 1 to determine the subsystem-level margins. Then the CCRS total system CBE can be computed per the last row in Table 5 and compared against the available total capture time from Figure 5e to determine the margin available, as reported in Table 7.

Table 5. Hardware Timing Performance Current Best Estimates

Item	Hardware Item	Timing CBE (s)	Subsystem Margin
1	Capture sensor electronics	0.050	100%
2	LTM swing arm	2.85	11%
3	Avionics	0.366	19%
CCRS System Total CBE:		**3.27**	

For metric 2, the CCRS total probability of success is based on the product of the reliability estimates and MC output as described in Section IIIc. To meet the ≥99.7% target $P_{S(total)}$ in metric 2, the allowable minimum probability of success for the system capability of 3.75 seconds along the total capture before bounce-back (Figure 5e) distribution is computable after accounting for the total probability of success of the components per Eq. 2. This minimum probability of success along the MC output distribution is indicated in the last row of Table 6, and its associated maximum probability of failure, $P_{f(MC)}$, is equivalent to $1\text{-}P_{S(MC)}$.

Table 6. Hardware Reliability Estimates

Item	Hardware Item	Reliability Estimate, P_s (%)
1	Capture sensor electronics	99.9999
2	LTM swing arm	99.95
3	Avionics	99.9923
	$P_{s(total)}/P_{s(MC)}$:	**99.9422**
	$P_{s(MC)}$:	**99.758**

Table 7. Capture Performance Results

Metric	Metric	Current Performance	Current Delta from (Table 3) Target	Details
1	**Percent System Margin Capture for Timing**	46% margin	+26%	• 0.13% from Figure 5e = 6.09sec
2	**Probability of successful capture**	3.75sec must be ≤0.242% on Figure 5e distribution	3.75sec is well below 0.13% on distribution	• 0.242%-ile = $P_{f(MC)} = 1 - P_{S(MC)}$

V. Conclusion

When the performance assessment of a technical parameter is complex and highly dependent on dynamic external interfaces, it is crucial to understand and properly represent the probability distributions for the inputs when ingesting them into the computations. This paper demonstrates a probabilistic approach using MC to assess the CCRS capture performance against self-derived targets. Similar thought processes can be applied to other non-traditional technical resources where performance targets are non-existent in the industry.

In the PDR-level assessment represented in this paper, each input parameter for the MC has conservatism baked into it, so any additional simplifying assumptions used to compute the capture-before-bounce-back time adds further margin that is not seen at the system-level. For instance, this study assumes that all rotational kinetic energy is converted to translational kinetic energy at first contact for all MC cases, which has some clear conservatism and built- in margin, and that the OS rebound velocity vector is in the worst-possible direction. The current target values for each metric, therefore, includes more margin than readily apparent. Future work, therefore, should consider refining and possibly reducing the target value for each performance metric identified to account for existing conservatism.

VI. Acknowledgments

The authors would like to thank the MSR, ERO, SRL, and CCRS project teams for their support and dedication to NASA's ongoing efforts to increase humankind's understanding of the universe. The decision to implement Mars Sample Return will not be finalized until NASA's completion of the National Environmental Policy Act (NEPA) process. This document is being made available for information purposes only.

VII. References

[1] Beaty et al. (2019). *The Potential Science and Engineering Value of Samples Delivered to Earth by Mars Sample Return*. Meteoritics and Planetary Science. Vol 54(3), pp 667-671.

[2] Haltigin et al. (2022). *Rationale and Proposed Design for a Mars Sample Return (MSR) Science Program.* Astrobiology. Vol 22(S1), pp S-27–S-56.

[3] Swindle et al. (2022). *Scientific Value of Including an Atmospheric Sample as Part of Mars Sample Return (MSR).* Astrobiology. Vol 22(S1), pp S-165–S-175.

[4] Grady et al. (2022). *The Scientific Importance of Returning Airfall Dust as a Part of Mars Sample Return (MSR).* Astrobiology. Vol 22(S1), pp S-176–S-185.

[5] Carrier et al. (2022). *Science and Curation Considerations for the Design of a Mars Sample Return (MSR) Sample Receiving Facility (SRF).* Astrobiology. Vol 22(S1), pp S-217–S-237.

[6] Cataldo et al. (2022 Sept 18-22). *Mars Sample Return – An Overview of the Capture, Containment, and Return System*. 73rd International Astronautical Congress (IAC). Paris, France.

[7] Sarli et al. (2023). *NASA Capture, Containment, and Return System: Bringing Mars Samples to Earth.* International Symposium on Space Technology and Science, Kurume, Japan.

[8] Geelen et al. (2021). *Mars Sample Return Campaign – Status of the ESA provided Elements*. 72nd International Astronautical Congress (IAC). Dubai, United Arab Emirates.

[9] Hanson and Beard. (2010 Aug 2-5). *Applying Monte Carlo Simulation to Launch Vehicle Design and Requirements Verification*. AIAA 2010 Guidance, Navigation, and Control Conference. Toronto, Ontario Canada.

[10] P. Wei et al. "Regional and parametric sensitivity analysis of Sobol' indices." Reliability Engineering and System Safety. Vol 137 (2015), pp 87-100, https://www.sciencedirect.com/science/article/pii/S0951832014003196.

[11] Saltelli et al. (2008). *Global Sensitivity Analysis: The Primer*. John Wiley & Sons.

[12] Gamboa et al. (2022). *Global sensitivity analysis: a new generation of mighty estimators based on rank statistics*. Bernoulli. Vol 28(4), pp 2345–2374.

[13] Cataldo et al. (2022). *Multifidelity uncertainty quantification and model validation of large-scale multidisciplinary systems*. Journal of Astronomical Telescopes, Instruments and Systems. Vol 8(3), pp 038001-1–21.